ISSN 0097-8078, Water Resources, 2014, Vol. 41, No. 7, pp. 819–832. © Pleiades Publishing, Ltd., 2014.
Original Russian Text © A.V. Anikeev, M.V. Leonenko, 2013, published in Geoekologiya, 2013, No. 2, pp. 130–146.

FUNCTIONING OF NATURAL AND NATURAL–ENGINEERING SYSTEMS

Forecast of Sinkhole Development Caused by Changes in Hydrodynamic Regime: Case Study of Dzerzhinsk Karst Area

A. V. Anikeev[a] and M. V. Leonenko[b]

[a] *Sergeev Institute of Environmental Geoscience, Russian Academy of Sciences, Ulanskii per. 13, bld. 2, Moscow, 101000 Russia*
E-mail: anikeev_alex@mail.ru
[b] *OAO Antikarst and Shore Protection, ul. Mayakovskogo 33, Dzerzhinsk, 606023 Russia*
E-mail: mvleonenko@mail.ru

Received November 22, 2011; in final form, May 24, 2012

Abstract—Data collected in the influence zone of a water intake near Dzerzhinsk City in Nizhni Novgorod oblast are used to demonstrate a close relationship between the frequency, intensity, on the one hand, and dimensions of karst sinkholes and three human-induced cycles of hydrodynamic regime 15, 13, and 12 years long, on the other hand. The approaches to and methods for local evaluation of territory stability at the local level are proposed, and the course of process development under the current geotechnical conditions is predicted. The results derived from some assumptions and the conclusions formulated in the article are supported by the volumetric rate of gypsum leaching in the area being relatively high.

Keywords: hydraulic pressure, hydraulic fracturing, gravity flow of granular solids, karst-suffosion hazard, groundwater pumping, sinkholes, mass suffusion, rock mass stability

DOI: 10.1134/S0097807814070021

INTRODUCTION

The active geotechnical studies of Dzerzhinsk region dates back to the late 1920s–early 1930s, when the chemical industry facilities, founded here before 1917, started rapidly developing. The city of Dzerzhinsk itself was founded in 1930 at the site of Rastyapino workers settlement and Chernorechenskaya railway station [10].

It became clear very soon that the construction site for major economic facilities has been chosen incorrectly by geological reasons. The result was that on May 10, 1941, USSR Council of People's Comissars (essentially, the Council of Ministers) adopted a resolution to create Dzerzhinsk Karst Station [11]. The obvious reason for such decision was the hazard of karst sinkholes. The World War II and the subsequent restoration of the country delayed the organization of this important institution by 11 years. However, since 1953, the geotechnical studies in the city and the region were largely determined by the operation of Dzerzhinsk Karst Station, USSR Academy of Sciences[1], which later was transformed into a subdivision of PNIIIS, USSR Ministry of Construction, and now exists as OAO Antikarst and Shore Protection.

[1] It was created by Savarenskii Laboratory of Hydrogeological Problems, USSR Academy of Sciences [10, p. 4].

Water intake of a chemical plant is situated on the left bank of the Oka R. 5 km northeast of Dzerzhinsk C. Its area is 3.4 km^2, and the area of its zone of influence, containing major industrial and transport facilities (Fig. 1) was as large as 30–31 km^2 in the mid-1970s. The 29 sinkholes that formed in the area in the last 40 years of the 20th century are now a

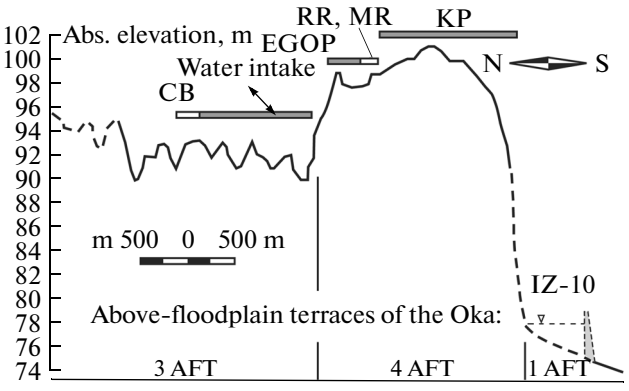

Fig. 1. Geomorphological profile of water intake zone of influence: CB is commodity base; water intake is water intake of water intake of Kaprolaktam Plant (KP); EGOP is ethylene and glycol oxide plant; RR and MR are Moscow—Nizhni Novgorod railroad and motor road; IZ-10 is IZ-10 sludge collector.

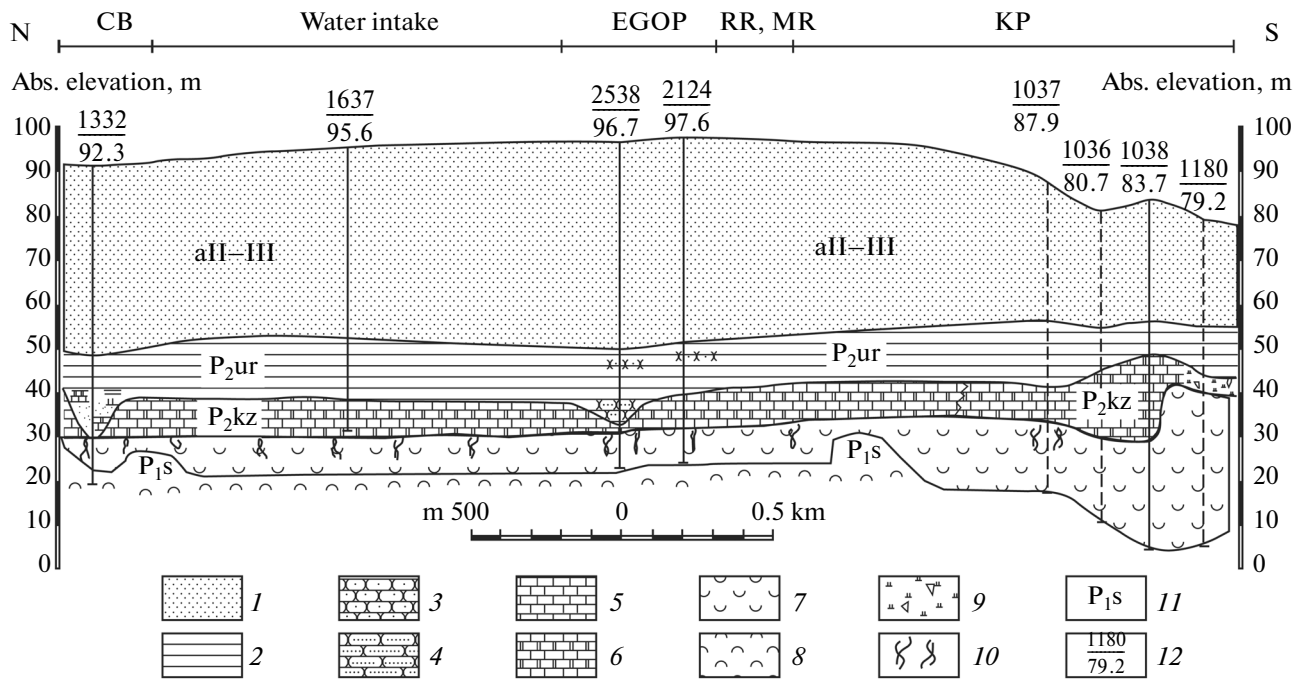

Fig. 2. Geological section: (*1*, *2*) sand and marl–clay strata, (*3*) aleurolite, (*4*) sandstone, (*5*) limestone, (*6*) dolomite, (*7*) gypsum, (*8*) anhydrite, (*9*) dolomitic powder with carbonate rock debris, (*10*) fracture porosity, (*11*) geological index, (*12*) well no. and abs. elevation of the well bottom. aII–III are alluvial deposits of the Middle and Upper branches of neo-Pleistocene. Permian system: P_2ur, P_2kz are the urzhumskii and kazanskii stages of the upper series, P_1s is the sakmarskii stage of the lower series.

major source of economic and environmental risk. In this context, the geotechnical conditions in the area and their long-term variations were analyzed in 2007 and the development of karst–suffosion process for period 2008–2010 was forecasted.

The following two sections of this article, in addition to the published literature, use materials of geological and geotechnical survey at scale of 1 : 200000, karst surveys, regime observations, and engineering surveys in the area available in the archive of OAO Antikarst and Shore Protection.

GEOTECHNICAL CONDITIONS

The area under consideration is situated within the third, fourth, and, partially, first above-floodplain terraces of the Oka R. (AFT) with absolute elevations of 89.0–96.0, 98.0–104.0, and 74.0–77.0 m, respectively [10]. The third and, to a lesser extent, fourth terraces have pronounced ridge–hill pitted relief (Fig. 1).

Quaternary Deposits

Down to the depth of 24–53 m, the massif is composed of alluvial accumulation of the middle and upper branches of neo-Pleistocene (aII–III), overlain on the surface by peat (1 AFT) and filled soils. The thickness of the latter is generally 0–3.5 m, though it increases to 10–15 m in ravines and funnels filled with soils.

Alluvial deposits are represented by fine and dust quartz sands, sometimes, medium-grained sands, with rare thin (0.5–0.8 m) lenses and interlayers of silty and sandy clays. Coarse sands with inclusions of gravel and pebble occur in the bottom part of the section, as is typical not only of this area [10]. The total thickness of the Quaternary, mostly sandy, stratum varies from 24.3 to 52.8 m (Fig. 2).

The coefficient of heterogeneity of the most widespread fine sands and their angles of slope in air-dry and water saturated state are K_h = 3.6–12.0, $(\varphi_0)_d$ = 27°–31° and $(\varphi_0)_w$ = 21°–29°. For dust sands, those characteristics are K_h = 2.8–5.6, $(\varphi_0)_d$ = 28°–37° and $(\varphi_0)_w$ = 27°–28°, and those for medium-grain sand are K_h = 3.0–8.4, $(\varphi_0)_d$ = 26°–32° and $(\varphi_0)_w$ = 24°–29°. The high values of K_h suggest the suffosion instability of sands, especially, fine sands, while the values of $\Delta\varphi_0 = (\varphi_0)_d - (\varphi_0)_w$, reaching 6°–9° in fine and dust varieties suggest their quicksand properties.

The mean values of the density of mineral part of sands are nearly the same: 2.65–2.66 g/cm^3. However, the density of those soils and their permeability vary widely. The coefficient of porosity of fine sands, depending on their dense or loose composition, varies within e = 0.49–1.48; that of dust sands, within e = 0.91–1.54, and that of medium-grain sands, within e = 0.44–0.63. The hydraulic conductivities of fine and dust sands with natural composition are K_{hc} = 1.06–3.26 m/day and K_{hc} 2.20–6.00 m/day, respec-

tively, and that in the medium-grain sands can reach $K_{hc} = 14.67$ m/day.

Permian Deposits

At the absolute elevations of 43.4–56.2 m, the Quaternary stratum is underlain by terrigenous deposits of urzhumskii stage, Middle Permian (P_2ur), commonly represented by red limestone clays and clayey limestones with bed of siltstones or, in the lower parts, sandstones. The cement of aleurolites and sandstones is calcareous–clayey; all rocks are gypsous [10].

Analysis of the columns of deep boreholes shows strong vertical and horizontal variations of the lithological composition of urzhumskie deposits. Their section most often entirely consists of clays and marls. Sometimes, the upper parts of the section is represented by aleurolites, which can also occur in the bottom of the stratum, and sometimes, they are represented by aleurites with clay beds. Sandstones are sometimes completely absent or form thin beds in the clay stratum, though their share in the total thickness of terrigenous stratum in borehole 2358 reaches 54%.

The zone of decomposed rocks up to 3.6–10.2 m in height and open cavities up to 0.5 m were revealed by drilling near the bottom of the stage. The former are represented by aleurites, sands, clay and aleurolite debris, landwaste and limestone dust, while the latter can be determined by sinks of the drill string. The total thickness of the urzhumskie deposits depends on the degree of their water erosion and the relief of the roof of underlying rocks. It varies from 1.0 m (borehole 20) to 18.9 m (borehole 1332), though, as a rule it does not exceed 7–15 m (Fig. 2).

The clays that dominate in the section show higher concentration of fine and dust particles (43.6–60.5%) and occur commonly in solid, semisolid, and tough state. The density of their matrix is ρ_d = 1.45–1.58 g/cm^3; $e = 0.73$–0.90, $K_{hc} = 1 \times 10^{-5}$–$2 \times 10^{-3}$ m/day for continuous and $K_{hc} = 5 \times 10^{-3}$–$7 \times 10^{-2}$ m/day for fractured varieties. In decompaction zones and in cavity walls, clays show plastic consistency and their density is low: $\rho_d = 1.31$–1.34 g/cm^3, $e = 1.04$–1.1. The strength of clays depends on their consistency. The adhesion and the friction slope of solid soils vary in the intervals $C = 63$–100 KPa, and $\varphi = 22°$–$24°$, while those for plastic soils vary from $C = 30$–35 KPa, $\varphi = 7°$–$14°$ to $C = 15$ KPa, $\varphi = 4°$.

Marls, whose important feature is the ability to soften in water, passing from solid to soft-plastic state, show the following characteristics: ρ_d = 1.42–1.94 g/cm^3, $e = 1.49$–1.83, $C = 41$–140 KPa, $\varphi = 6°$–$28°$. The properties of aleurolites and sandstones are determined by their composition and the state of cement; therefore, they vary within wide ranges K_{hc} = 0.006–1.4 m/day, $C = 7$–65 KPa and $\varphi = 23°$–$39°$.

At absolute elevations of 32.6–48.7 m, marine deposits of kazanskii stage, Middle Permean (P_2kz) occur, represented by organogenic dolomitic limestones and fine silicified dolomites with subordinate beds of calcareous clay and clay marls. Carbonate rocks are cavernous, fractured, gypsum-containing, sometimes destroyed to rubble, debris, and dust. The thickness of destroyed zones varies from 0.1–0.4 m to 5.8–6.4 m. Open karst cavities 0.3–1.5 m in height and closed ones (2.4–5.4 m) occur, a fact that is in general agreement with data obtained for the entire Dzerzhinsk district [10, pp. 84–85]. The underground forms are most often filled with sand, dolomite powder, aleurolite debris with aleurite inclusions, and limestone debris.

The thickness of kazan deposits varies within 0.0–20.4 m. Their thickness is maximal in the zones of underlying-rock erosion. Here, in addition to lower elevations of the floor, higher elevations of the superface of the stage were recorded (Fig. 2). The absence of carbonate rocks and their low (down to 0.0–1.0 m) thickness are due to the development of karst and erosion processes at the boundary between the kazanskii and urzhumskii ages [10].

The most ancient deposits penetrated by boreholes at absolute elevations of 26.1–40.0 m were gypsums and anhydrites of sakmarskii stage of Lower Permian (P_1s). Fractured cavernous gypsums with a thickness of 0.0–13.0 m compose the top of the section (Fig. 2), where core recovery ratio sometimes drop from its common values of 80–90% to 50–60%. Borehole 1180, at marks of 33.2–32.2 m, crossed a cavity, filled with gypsum detritus, earthy gypsum, and coarse sand. Anhydrites are cryptocrystalline dolomitic, monolith, strong, sometimes alternating with gypsums. The thickness of the bottom layer penetrated by the borehole reaches 14.6 m.

Thus, the analysis of geotechnical conditions shows that Quaternary sands are apt to fluidization and are unstable in terms of suffosion. Processes of caving, accompanied by the formation of intermediate cavities, took place in the shielding urzhumskie deposits. The carbonate rocks of kazanskii and the gypsums of sakmarskii stages can accumulate crashed connected and disconnected soils from overlying strata. Since the rate of gypsum dissolution in this area is high enough [8, 9], it is safe to say that the processes of caving clays and the formation of karst cavities, which accumulate debris, developed not only in geological, but also in historical time.

Hydrogeological Conditions

Alluvial sands contain unconfined aquifer with absolute elevations of subsoil water level (SWL) varying from 87.0 in the northern to 73.0 m in the southern part of the area. The thickness of the horizon in this direction decreases from 36–38 m to 18–19 m. The major drain is the Oka R. The subsoil water (SW) is recharged by infiltration of atmospheric precipitation, and leakages from settlers and water conduits. By their chemistry, the waters are sulfate–hydrocarbonate cal-

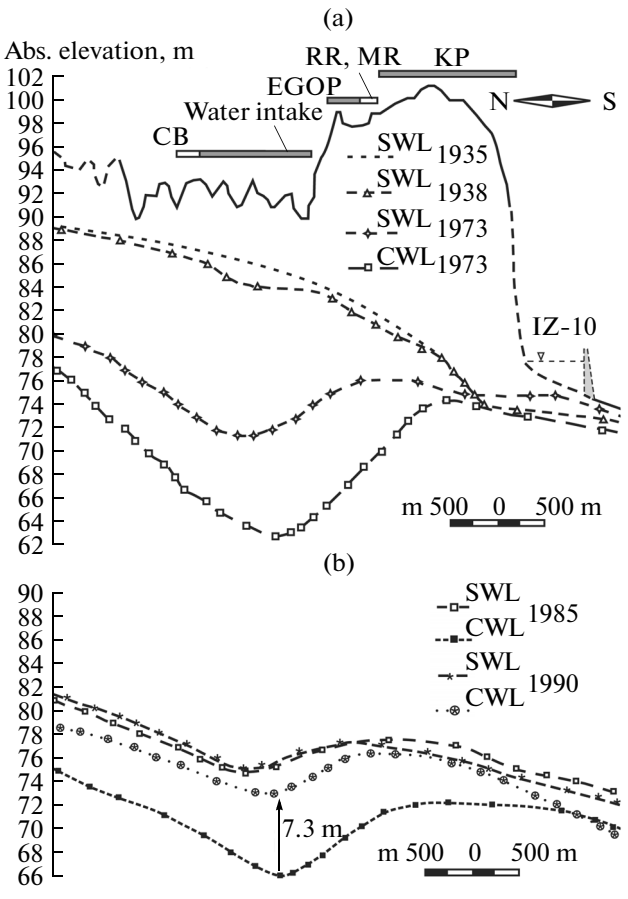

Fig. 3. (a) Positions of the levels of subsoil (SWL) and confined fracture–karst (CWL) waters in 1935, 1938, and 1973 and (b) the shape of depression cones in 1985 and 1990. Other denotations see Fig. 1.

cium and sodium–calcium with mineralization from 0.11 g/L at the water intake site to 0.41–0.63 g/L at some distance from it.

A system of confined fracture–karst waters (CW) with a thickness of 3.0–20.1 m lies in Permian sandstones, limestones, dolomites, and gypsums. The piezometric level (confined-water level or CWL) keeps at elevations of 85.0–86.0 m in the northern and 68.0–70.0 m in the southern part of the territory. The top aquiclude, which separates this system from unconfined water, is represented by clay deposits of the Middle Permian; while its bottom aquiclude, by anhydrites of sakmarskii stages, and rarer, monolithic gypsums or clays and marls lying in the basement of the kazanskii stage. Waters are sulfate–carbonate magnesium, carbonate magnesium, or sulfate calcium with mineralization of 1.55–2.46 g/L.

Groundwater regime changed considerably in the late 65 years of the XX century. Below, an attempt is made to describe the changes in the hydrodynamic regime alone and to demonstrate their direct correlation with the character and intensity of karst–suffosion process.

GROUNDWATER LEVEL DYNAMICS AND SINKHOLE FORMATION

Changes in Hydrogeological Conditions

Groundwater pumping tests in the water intake area started in 1935. Before this, SWL varied from 88.0–89.0 m north of Commodity Base (CB) to 73.0 m south of IZ-10. According to data in [10], CWL was close to SWL; therefore, it was assumed that, initially, their difference never exceeded 1–2 m (Fig. 3a). By 1938, the rate of SW withdrawal had reached 1.5×10^5 m^3/month, resulting in the formation of a small depression on groundwater table. The clear bend in SWL in the south is due to a drop in land surface elevations, which causes an increase in surface runoff and a decrease in the infiltration of rain and snowmelt water in the slope of the 4th AFT (Fig. 3a). Later on, the annual yield of the wells tapping the top aquifer gradually increased from 2.1×10^6 m^3 in 1939 to 8.9×10^6 m^3 in 1960. The only exception was period 1943–1948 when it was not higher than $(3.6–4.2) \times 10^6$ m^3/year.

In 1961, pumping of fracture–karst water began, and the withdrawal of SW somewhat decreased, varying within $(7.2–8.4) \times 10^6$ m^3/year until 1967. CW consumption increased from 1.6×10^6 m^3 in 1962 to 6.0×10^6 m^3 in 1970; only in 1964, it temporarily decreased to 1.3×10^6 m^3. The result is that, by the mid-1970s, SWL in the center of water intake has dropped by 17 m and CWL, by 22 m; deep depression cones have formed at the boundaries of the 3rd and 4th AFT, and the area of influence of the water intake has increased to 30–31 km^2. Contrary to that, SWT at the 1st AFT increased by 1.5–2 m because of leakage from IZ-10 settler, which has been constructed near the southern boundary of ZK, and the underflooding of this area (Fig. 3b).

According to data of many-year observations, the largest difference of heads, $\Delta H = 10$ m, was recorded in 1973. However, all measurements were carried out every year in late August. As can be clearly seen in Fig. 4, this is the period when the difference between piezometric level is minimal, since in summer and early autumn, the yields of shallow production wells regularly increased by $(5–10) \times 10^5$ m^3/month, while that of deep wells often decreased. The head difference always reaches its maximum in late autumn, winter, and early spring, and in this period of 1973, it could reach $\Delta H = 14–19$ m.

In fact, the most hazardous was the situation not in 1973, but in 1969, when the consumption of fracture–karst water increased and that of subsoil water decreased, and the annual discharges of wells tapping those aquifers became nearly equal (Fig. 5). In the early 1969, as it was shown by the analysis of pumping rates, the rate of SW withdrawal was even less than that of confined water by 150000 m^3/month (Fig. 4). In this period, the level difference, according to our estimates, was $\Delta H = 20–25$ m.

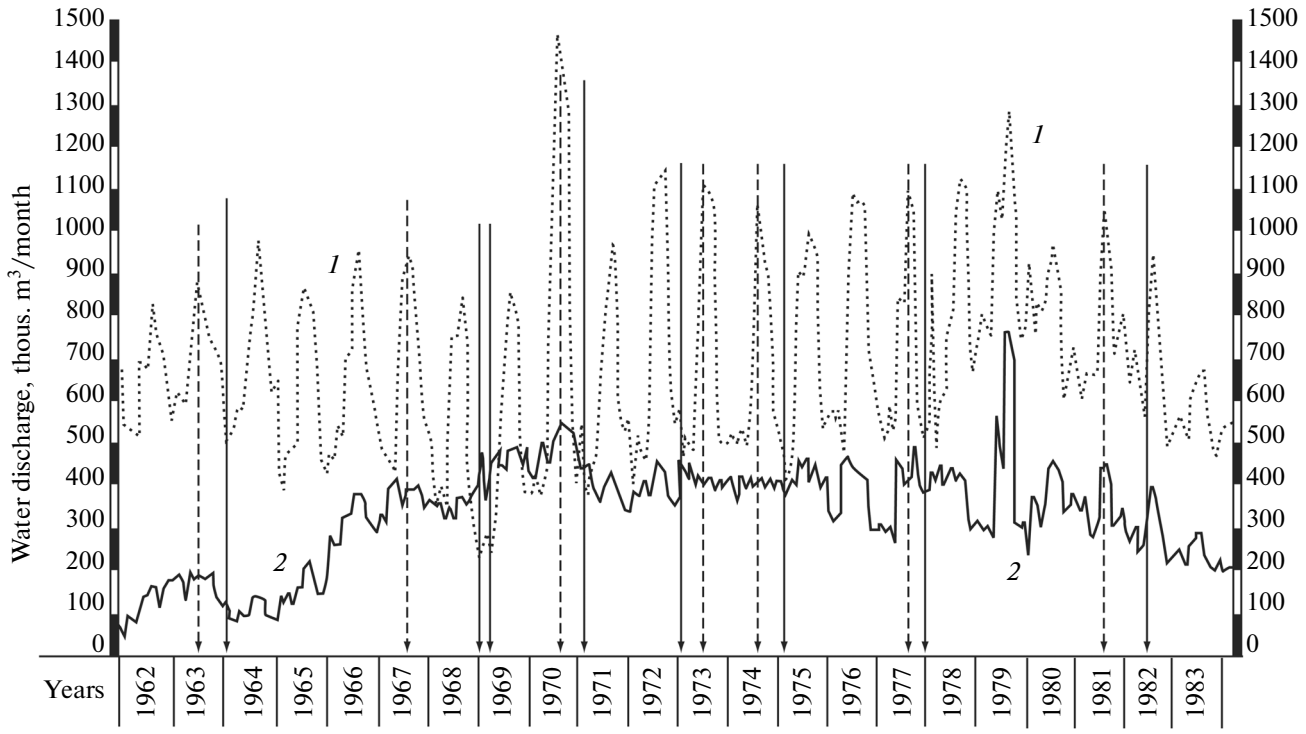

Fig. 4. Pumping rates of (*1*) subsoil and (*2*) fracture–karst waters in 1962–1983. Full and dashed arrows show the moments of maximal and minimal differences between the piezometric levels.

In 1979, the consumption volumes of SW and CW increased to $Q_s = 12.6 \times 10^6$ m^3/year and $Q_c = 5.7 \times 10^6$ m^3/year, after which they started decreasing with approximately the same rates ($Q_s/Q_c = 2.2–2.3 \approx$ const, Fig. 5). In 1985, when they decreased to $Q_s = 6.2 \times 10^6$ m^3/year and $Q_c = 2.6 \times 10^6$ m^3/year, the top and bottom depression cones became shallower by 4 and 3 m compared with 1973, respectively (see Figs. 3a, 3b).

The quite regular relationship between the rates of pumping and the position of groundwater levels was sometimes violated because of the uneven operation of the municipal water intake, situated 3.5 km northwest of CB site. Thus, in 1990, water consumption decreased to $Q_s = 4.6 \times 10^6$ m^3/year, $Q_c = 1.9 \times 10^6$ m^3/year, the amplitude of CWL rise was 7.3 m, while SWL rose by as little as 0.5–1 m (Fig. 3b). However, of greatest importance for us is that the difference between the heads decreased by about $\Delta H = 6.5$ m. The effect of water intake of Dzerzhinsk C. can also be seen in Fig. 3a in the low elevations of the northern wings of depression cones.

In 1992, the discharge of operation wells again increased ($Q_s = 5.5 \times 10^6$ m^3/year, $Q_c = 2.7 \times 10^6$ m^3/year). In the center of the bottom funnel, the elevations of its bed dropped by 2 m compared with 1990, while those on the axis of the top funnel rose by 0.5–1 m (Figs. 3b, 6a), and the difference between the levels again increased by about $\Delta H = 3$ m.

In the subsequent years, the pumping rates of SW and CW gradually decreased. An insignificant increase in the volumes of extracted water in 1997 and 2005–2007 causes no significant perturbations in the general pattern of level variations, which is given in Fig. 6. It can be seen that by the late 1990s, the depression cones nearly disappear (Fig 6a). In the early XXI century, groundwater levels continue gradually recovering, though not reaching the original elevations in the major portion of the territory (Fig. 6b).

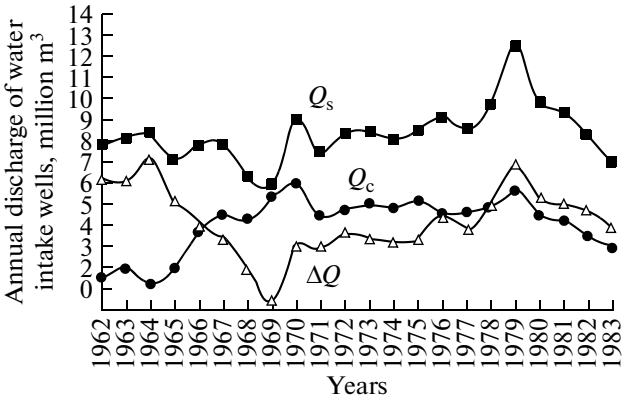

Fig. 5. Time variations in the well discharge rates (Q) and the difference between such rates ($\Delta Q = Q_s - Q_c$) for wells developing subsoil (Q_s) and confined (Q_c) waters.

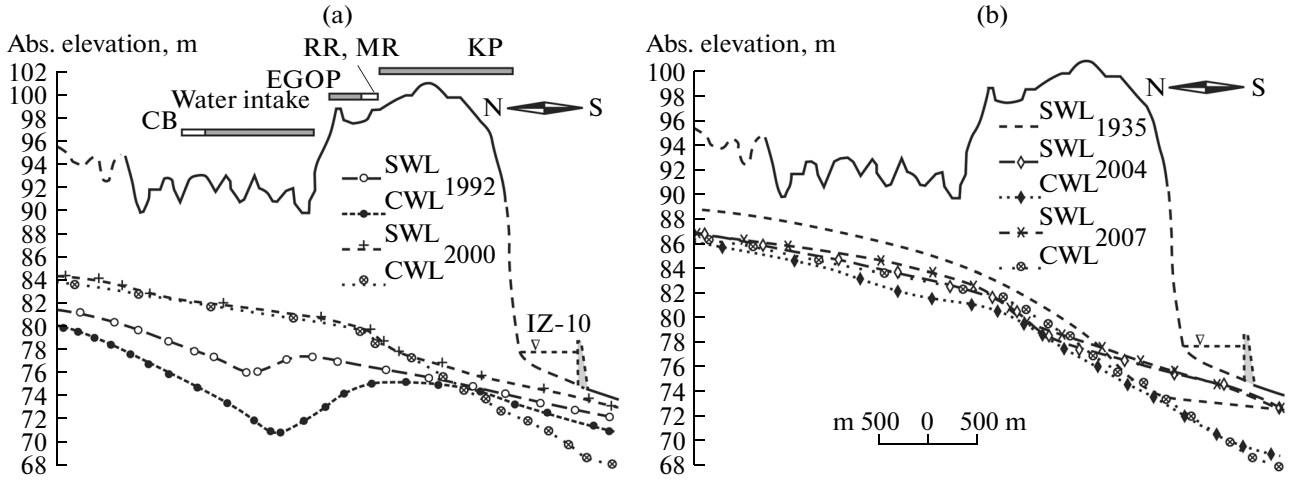

Fig. 6. The character of groundwater level recovery in the late XX–early XXI centuries; (a, b) see explanations in the text.

Technogenic Intensification of Karst–Suffosion Process

The first sinkhole with a depth $h_c = 2.2$ m and diameter of $D_c = 6.2$ m formed almost 500 m west of the water intake in 1960, when the pumping of fracture–karst water has not started, and the drawdown of SWL was only 8–8.5 m (Fig. 7). The second funnel ($h_c = 0.6$–0.8 m, $D_c = 4.4$ m) formed at the water intake site 6 years after the development of CW began and long before the maximal drop in SWL and CWL. It is only the third funnel ($h_c = 2.5$ m, $D_c = 12.8$ m) that formed in 1975, when level elevations became minimal. The other 26 sinkholes (18 in the water intake area and 8 at nearby areas) appeared in the period when groundwater levels were recovering (Fig. 7a). It is the likely cause of the great attention paid to the effect of this hydrogeological process on the stability of karstified areas in [30, 31]. Note that until 1960, this site was regarded as safe in terms of karst and suffosion [10, 25].

In our opinion, Fig. 7b contains much more information than Fig. 7a, as the head difference between subsoil (H) and fracture–karst (H_0) waters ($\Delta H = H - H_0$) characterizes their force impact on rock massif:

$$p_d = I\gamma_w = \Delta H\gamma_w/m, \quad (1)$$

where p_d is hydrodynamic pressure, I is the gradient of vertical groundwater flow, $\gamma_w \approx 10$ kN/m^3 is water density, m is the thickness of clay rocks of urzhumskii horizon, and there are no when such rocks, the thickness of water-saturated sands. As follows from (1), other conditions being the same, in particular, at $m = \text{const}$, the value of ΔH fully determines the value of p_d.

The plots in Fig. 7b clearly show three cycles of increase and decrease in ΔH with a duration of 15, 13, and 12 years, characterized by a gradual decrease in the technogenic load onto the rocks. The values of $\Delta H = 14$, 12, and ≤ 8 m, shown in Fig. 7b should be considered as the maximal possible values. The three cycles are preceded by the stage 1935–1960, when the downward hydrodynamic pressure decreased to zero and even negative values. It is this period when, because of the ascending water flow and weakening structural bonds and friction forces in loose soils, the first sinkhole formed. The formation of this, as well as the second sinkhole long before the peak values of hydrodynamic pressure have formed, appears to have been prepared under undisturbed conditions; therefore, they cannot be referred to as background or natural–technogenic manifestations of karst–suffosion process. For the rest 27 cases, a clear correlation can be seen between the three cycles of anthropogenic impact and the number, mean size, and formation frequency of surface forms; therefore, they can be referred to technogenic sinkholes.

The latter conclusion is supported by the distribution character of sinkholes over seasons. Thus, out of the 20 funnels with known appearance date, 30% of cases fall on November–February, i.e., the period quite unusual for them to form. However, in this period, as shown above, the head difference in groundwater reached its maximum. If we exclude the first two sinkholes, referred to as background, the contribution of purely technogenic manifestations of the process becomes even more—50%.

At the end of the first cycle (1961–1975), only two sinkholes with maximal diameter $(D_c)_{max} = 12.8$ m were recorded; however, conditions for their formation in the future were formed. During the second cycle (1976–1988), the hazard reaches its peak (18 sinkholes, $(D_c)_{max} = 14.5$ m). During the third cycle (1989–2000), the force impact decreases considerable, as does the hazard (sinkholes, $(D_c)_{max} = 6.0$ m), and there are no manifestations on land surface since 1999 to 2007 (Fig. 7).

Questions arise: what took place during those cycles of anthropogenic load onto subsurface hydro-

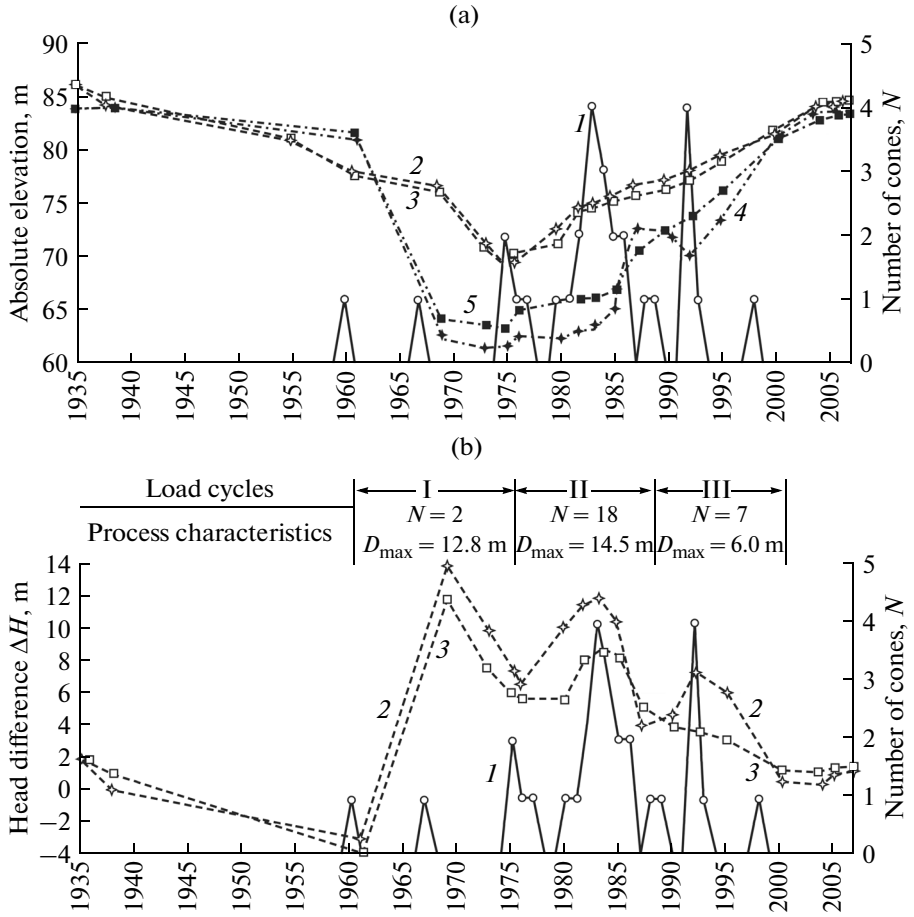

Fig. 7. Time variations in (*1*) (a, b, right axis), the number of sinkholes, (a) (*2*, *3*) the level of subsoil and (*4*, *5*) the head of fracture–karst waters, and (b) the difference between piezometric levels. (a) (*2*, *4*, and *3*, *5*) By measurements in observation wells 52, 52a, and 186, 186a, respectively; (b) (*2*, *3*) difference between heads in wells 52, 52a and 186, 186a; D_{max} is the maximal diameter of sinkhole.

sphere, how the stability of the massif was disturbed, and what should be expected after groundwater levels approaching their initial position? Below we answer those questions.

FORECASTS OF SINKHOLE FORMATION

Retrospective Analysis and Prediction of the Stability of Urzhumskii Stage Deposits

The conclusion that it was the first cycle of technogenic load that has provoked the rapid development of sinkholes is based on the results of not only the analysis of groundwater dynamics and the character of sinkhole formation, but also on evaluation of the stability of low-permeability rocks at an accidental hydraulic fracturing. The concept of this process has formed in the course of its laboratory and field studies in the 1980s–1990s [1–4]; now it is studied by mathematical simulation [41].

We will consider only the essence of the phenomenon and the new aspects of the problem. We faced them in recent years, when analyzing studies (far from new, but still important) of mining engineers and geomechanic experts [18, 19, 21, 22, 32–34, 36, 41].

It was found that a decrease in the formation pressure causes an ejection of rock fragments from the bottom of the shielding layer, its fracturing along a system of break surfaces, and a rapid propagation of the breakage front from the bottom to the top. Figure 8a shows that, once a layer is destroyed, the debris fill small cavity, and the process ceases. When a cavity forms (Fig. 8b), the destroyed clays, and next, overlying sands enter the fracture–pore space of karstified rocks, and, we see an increase in the domain of their release and decompaction forms in loose soils, a process the effect of which appears later on the land surface. Under the conditions under consideration, this can be caused by not only mechanical export of the material that fills the cavity, but also by an increase in its size due to rock leaching.

Analysis of the complex interaction between pore water and rock matrix yielded simple formulas (2) and (3), relating the critical head difference (ΔH_{cr}) with engineering–geological characteristics of soils [4]:

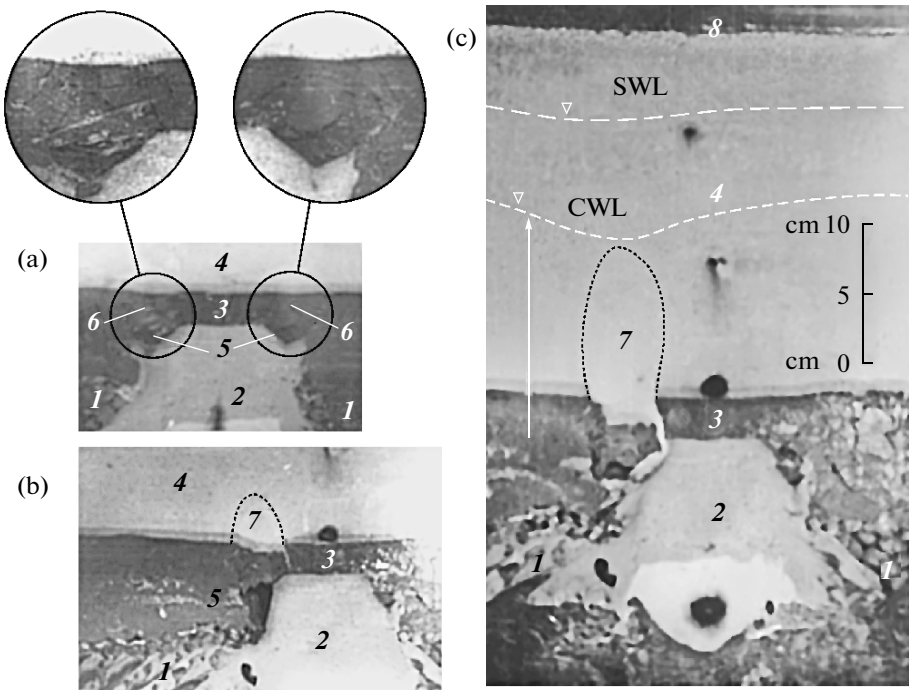

Fig. 8. Hydraulic fracturing of (a) shielding clays and (b, c) its consequences. The result of simulation by the method of water-saturated equivalent materials: (*1*) karst rocks, whose fracture–pore space is the accumulation domain of debris; (*2*) zone of weakening of the massif (paleoincision, ancient collapse, etc.); (*3*) low-permeability bed; (*4*) loose soil stratum; (*5*) cavities; (*6*) crushed-clay areas; (*7*) sand decompaction zone; (*8*) day surface. SWL, CWL are the levels of subsoil and confined fracture–karst waters, respectively.

$$\Delta H_{\text{cr}} = C/n_e\gamma_w, \quad (2)$$

$$\Delta H_{\text{cr}} = (C/\gamma_w + m)/n_e, \quad (3)$$

where n_e is the effective porosity. Equation (2) determines the minimal head difference, which initiates hydraulic fracturing in low-permeability rocks, corresponds to the static condition of abrupt release of coal and gas from the surface opened during tunnel driving [18, 19, 36]. Formula (3) establishes the value of ΔH at which a through hole forms in the aquiclude, if the initial piezometric levels had nearly the same elevations ($H \approx H_0$; $-0.1 \le I \le 0.1$).

Basing on the present-day concept of water types in soils, the conditions of its formation, structure, and properties [7], we will consider bound water as an integral part of soil matrix, while its other categories will be referred to fluid component. This approach is even more appropriate, considering that, in this case, the effect of water flow on the mechanical interaction between the solid and liquid phase of the soil can be neglected, since, as well as in the case considered in [35], the forces of normal pressure of liquid are much greater than the forces of viscous friction [1]. Now, considering that the total amount of water of polymolecular adsorption is characterized by maximum hygroscopic moisture capacity w_{mg}, and soil moisture content is $S_r = w\rho_d/n\rho_w$, we obtain

$$n_e = (w - w_{mg})\rho_d/\rho_w S_r = n(w - w_{mg})/w, \quad (4)$$

where $\rho_d = \rho/(1 + w)$ is the density of rock matrix (ρ is soil density, w is natural moisture content).

Unfortunately, the maximum hygroscopic moisture capacity cannot be determined at standard geotechnical conditions. It also can be rarely determined even in special studies [17]. Even the author of the serious study [37], when analyzing the structure, composition, and storage properties of clays, deals with its hygroscopic moisture content; therefore, it was assumed that $n_e \approx n$, while in fact, $n_e < n$, and, hence, the estimated ΔH_{cr} is less than those required for destruction. By their grain size distribution, clay deposits of the Middle Permian belong to loams, for which $w_{\text{mg}} \le 4$–7%, an assumption not very rigid, in the authors' opinion. Taking into account the high rate of gypsum dissolution, shown in [8–10], it appears even more reliable, since the values of ΔH_{cr} above large holes is less than those derived from (2), (3).

Table 1 gives characteristics of the properties of different types of soils, composing the low-permeability stratum of the urzhumskii stage, and the results of their stability calculations by (2). It can be seen that all low-permeability rocks have been subject to hydraulic fracturing to some extent. The clays could be destroyed, in particular, in the marginal parts of depression cones, while aleurites showed no resistance to this process. The most stable were marls and

Table 1. Properties of rocks of urzumskii stage and failure head differences

Rocks		Porosity n, fractions of unit	Adhesion C, kPa	Pressure difference according to (2) ΔH_{cr}, m
Clays	Tough	0.47	(30–35)/32	6.8
	Plastic	0.52	15	2.9
Marls		0.45	(41–140)/60	1.3
Aleurolites		0.40	(35–45)/40	1.0
Aleurites		0.38	(5–7)/5	1.3

The top numbers are limiting values, the bottom numbers are calculated values.

aleurolites; however, even they could not resist fracturing at water intake site.

We will base our study on the physicochemical characteristics of clays, as they dominate in the shielding stratum. We assume that, originally, they were tough. If the technogenic load during the first cycle was not enough for hydrogeological windows, then, in accordance with process features, we assume that the consistence of clays above the weaker rock massif parts has become plastic.

The results of calculations show that in 1961–1975, through holes in an aquiclude formed in the places where its thickness was not greater than 7.6 m in the central part of the area and 2.4 m in its periphery (Table 2). Similar values of the critical thickness (6.3 and 2.7 m) were obtained for the second cycle. At the third stage, those values decrease appreciably, but the total thickness of crushed soils in the center of depression cones (16 m) is close to the largest thickness of urzhumskaya stratum (18.9 m). In their marginal parts, the thickness (5.2 m) approaches the most widespread values of layer thickness (7–15 m).

Thus, throughout period 1961–2000, through holes in the aquiclude could appear not only in water intake site. However, they cannot be expected to appear now, considering, on the one hand, the relatively high critical difference of heads and, on the other hand, the specific features of hydrodynamic regime at the boundary between the XX and the XXI centuries.

Prediction of Sinkhole Diameters and Their Formation Rates

The above reasoning suggests that, under current conditions, the main role in the formation of sinkholes belongs not to forced destruction of soils, but to the karst process proper, as well as suffosion, i.e., leaching of soluble rocks, erosion and redistribution of materials filling the fracture–pore space, and export of Quaternary sands into karst collectors. The conclusion of the authors of [20] that the domain of suffosion export is the Oka R. is not well founded in the authors' opinion. A.P. Kapustin wrote about the negative effect of this misconception as far ago as 50 years [10, p. 55].

Different approaches are used to give a quantitative description to the mechanism of effluence of loose soils into subsurface cavities [5, 6, 12–16, 23, 24, 26–28, 30, 31, 38–40, 42]. Its qualitative, verbal descriptions are much more numerous. Our forecast is based on the concept of the influence domain of a weakened area, which is described in detail in [3–5]. Here, we remind its major concepts and show its possible practical applications.

Scheme in Fig. 9 reflects the fact that, near a cavity, rock massif has an internal structure, which forms as the result of self-organization of the geological environment. The scheme is a good illustration of the above concept. The scheme and the concept are based on the notion of changes of the stress-strain state of rocks and interaction between zones of active and passive pressure near a karst cavity, dynamic dome, block deformation, localization of deformations, and basic properties of loose soils, i.e., the friction and dilatancy [3, 6, 12–16, 23, 24, 26, 27, 38–40, 42].

In the section, the boundaries of the ellipsoid and the zones it consists of smooth curves describing a combination of polygonal lines (Fig. 9). The latter consist of lines of active ($\beta = \pi/4 + \varphi/2$) and passive

Table 2. Limiting values of the thickness of sealing clays in accordance with equation (3) at different stages of technogenic impact

Time and place ((1) center of the water intake, (2) marginal parts)		Head difference ΔH, m	Porosity n, fractions of unit	Adhesion C, kPa	Thickness m_{cr}, m
I cycle,	1	(20–25)/23	0.47	(30–35)/32	7.6
1961–1975	2	(10–15)/12			2.4
II cycle,	1	(14–16)/15			6.3
1976–1988	2	(6–10)/8	0.52	15	2.7
III cycle,	1	(5–9)/7			2.1
1989–2000	2	(2–5)/3			0.1
Total thickness of clays destroyed in 1961–2000				max (1)	16.0
				min (2)	5.2

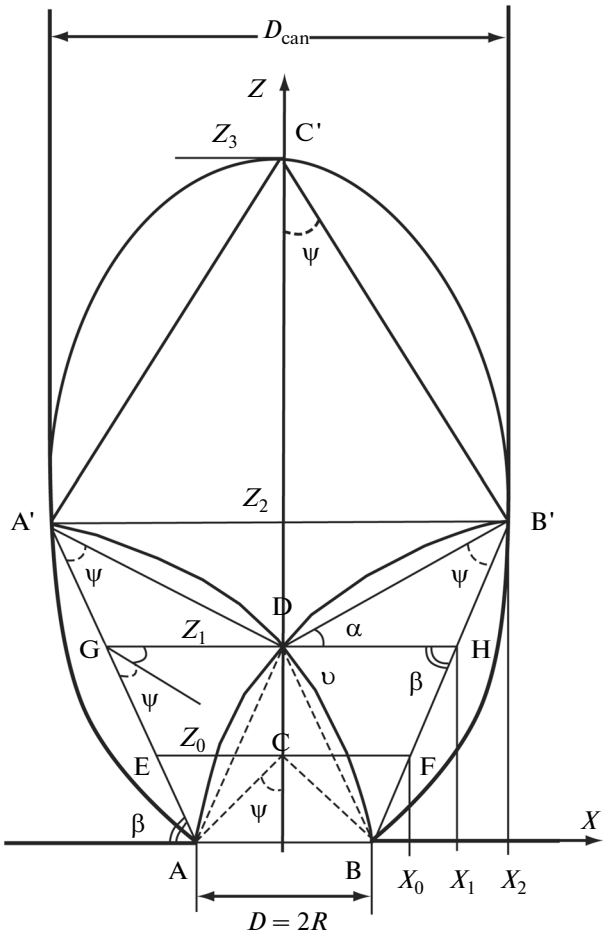

Fig. 9. Zonal structure of the influence domain of a karst cavity AB for the case where the blanket stratum is composed on loose soils: ACB is a zone of full rock movement or falling dome (the zone of free falling of particles in the regime of fast outflow of granular solids): ADB is the zone of stress removal, decompaction, and potential collapse in statics, in dynamics—the zone of predominant collision of particles; AA'DB'BDA is the zone of support resistance and possible slip (dynamic zone of plastic flow); AA'DB'B is dynamic dome; DA'C'B'D is the transition zone from anomalously low and high stresses to lithostatic stresses (the zone of possible bending and decompaction in statics and the zone of transition from converging movement to piston-like in dynamics); AA'C'B'B is the zone of influence of a weakened zone or release ellipsoid in the regime of rapid motion; $\alpha = \pi/4 - \varphi/2$; $\beta = \pi/4 + \varphi/2$, $\psi = \varphi$, $\upsilon \approx \varphi/2$, φ is friction slope; D_{can} is the diameter of sand flow canal.

($\alpha = \pi/4 - \varphi/2$) pressure, as well as segments of straight lines AC, AD, along which shear strains are localized, not only near the hole, but throughout the canal where granular or crushed rocks are moving. We emphasize that the dimensions of the channel are fully determined by the dimensions of the influence zone. The slopes ψ, υ of lines AC, AD are also functions of the friction slope: $\varphi = \varphi'_\mu + \nu$, where $\nu_{min} \le \nu \le \nu_{max}$ is the dilatancy level, associated with particle packing and changing at deformation; φ'_μ is the angle of contact or effective friction of a granular material for which $\nu = 0$.

The inconstancy of the friction angle hampers the interpretation of the process; therefore, in the practice it is advantageous and quite admissible to use the values of φ_{min} or φ_{max}, depending on the properties and state of loose soils. Those values can be readily found from the value of residual shearing resistance or peak strength, and, as a first approximation, they correspond to the slope angles of the maximally loose and dense compositions.

Geometric construction alone yield (Fig. 9)

$$D_{can} = 2x_0 = 2R/\sin\varphi, \quad (5)$$

$$z_0 = R/\tan\psi = R/\tan\varphi, \quad (6)$$

$$D_{can} = 2x_1 = R(1 + \sin\varphi)/\sin^2\varphi, \quad (7)$$

$$z_1 = R/\tan\upsilon = R(1 + 2\sin\varphi)/2\tan\varphi\sin\varphi, \quad (8)$$

$$D_{can} = 2x_2 = R(1 + \sin\varphi)^2/2\sin^3\varphi, \quad (9)$$

$$z_2 = z_1 + R(1 + \sin\varphi)/4\tan\varphi\sin^2\varphi, \quad (10)$$

$$z_3 = z_2 + x_2/\tan\varphi. \quad (11)$$

Equations (5)–(8) determine the dimensions of the influence domain at the stage of transient motion and (9)–(11), at the stage of steady-state motion. Here, $D_{can} = 2x_0$ is the maximal possible width of the canal at the first form of sand motion ($D \le D_{can} \le 2x_0$), and $D_{can} = 2x_1$ and $D_{can} = 2x_2$ are its maximal and minimal diameters, if the second form is realized ($2x_1 \le D_{can} \le 2x_2$). Equations (5), (7), (9) allow one to solve the inverse problem of evaluating the span of the hole D in the base of the sand stratum by known values of diameter of new funnels ($D_c \approx D_{can}$). This problem is also of interest from the viewpoint of organization of geophysical studies and the identification of sites where sinkholes can form.

As shown in the first section of this article, fine sands, which dominate in the section of Quaternary deposits, weakly resist suffusion and can liquefy. Moreover, it can be claimed a priori that, despite the considerable past drop of SWL, the domains of influence of karst or intermediate cavities always kept under water. In this context, we suppose that, whatever the compaction density and the rate of effluence of loose soils, the second form of their motion will realize with maximal canal diameter (9) and assume for calculations the values of the natural slope of fine water-saturated sands $(\varphi_0)_c$.

Equation (9) can be rewritten as

$$D = 4D_{can}\sin^3(\varphi_0)_c/(1 + \sin(\varphi_0)_s)^2, \quad (9a)$$

where $D_{can} \approx D_c$ is the diameter of new funnel. The results of determination of the width of weakened areas in accordance with available data on $(\varphi_0)_c$ and D_{can} are given in Table 3. It can be seen that the values

of D vary within a wide range (0.1–3.0 m), though they are not large in terms of their absolute values. This, in combination with the large thickness of the blanket stratum, can be the cause why intermediate cavities are difficult to detect by geophysical methods.

The mean maximal value $D = 2$ m appears to be typical of the first two cycles of technogenic impact, when the funnels were large and the process of roof collapsing was the main mechanism of sinkhole formation. Narrow canals of sand flow can form in the clays that had been disintegrated (see Fig. 8), the width of the canals being determined by the mean minimal value $D = 0.5$ m (Table 3).

Forecasts of dimensions of karst–suffosion funnels show (Table 4) that, under current geotechnical conditions, the mean diameter of sinkholes can be expected to decrease almost by half and the maximal diameter, by a factor of three. Conversely, the minimal diameter will increase by almost 2.5 times (Tables 3, 4). Thus, the scatter of D_c will decrease by five times and the size of funnels will generally decrease.

The cumulative curve of sinkholes in Fig. 10 allows regularities in the time variations of process frequency to be identified and the future values of this characteristic to be assessed. Its step-wise shape is very similar to the shape of rheological curves, in which the stages of preparation, progressing development, and attenuation of deformations can be isolated. Connecting the base and the rear seam of each step by straight lines, we obtain a polygonal line. The slope ratio of its segments is the frequency of formation of surface forms at different stages of sinkhole formation. The first six ones, pairwise almost coincide in time with the three cycles of technogenic load. The slope of the last, seventh, segment can serve as a forecast characteristic of the most pessimistic scenario of the karst–suffosion pro-

Table 3. Results of calculations of span D of weakened areas in the foot of sand stratum by (9a) as a function of the slope angle of fine water-saturated sands φ_0 and the diameter of karst–suffosion sinkholes

Characteristic / Values	φ_0, deg	D_c, m	D, m	Mean values of D, m	
Minimal	21	1.0	0.1	0.5	
Mean	25	6.2	0.9		
Maximal	29	14.5	3.0		2.0

Table 4. Diameter of sinkholes that can form under current conditions

Slope angle of water-saturated sands φ_0, deg		Mean width of cavities in the foot of sands D, m	Forecasted values of sinkhole diameter, D_c, m	
Minimal	21	0.5	Maximal	5.0
Mean	25		Mean	3.4
Maximal	29		Minimal	2.4

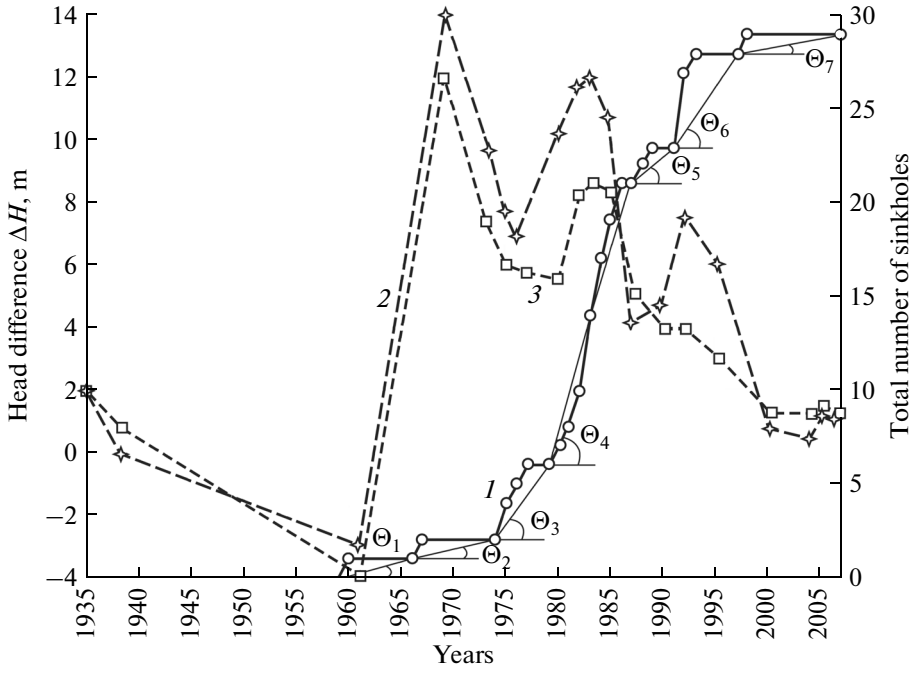

Fig. 10. (*2*, *3*) Dynamics of force impact of groundwater and (*1*) an increase in the total number of sinkholes over time: $\tan\theta_i = (N/T)_i$ is sinkhole formation frequency; $i = 1, 2, \ldots, 7$ are process stages; $\tan\theta_7 = 0.1$ year^{-1} is the maximal possible frequency of sinkhole formation for the most pessimistic process development scenario in 2008–2010. Other denotations see in Fig. 7.

Table 5. Stages of sinkhole formation and their characteristics (N/T is the frequency, $\lambda = N/ST$ is the rate of the process)

Stages	1	2	3	4	5	6	7
years	1959–1966	1967–1974	1975–1979	1980–1987	1988–1991	1992–1997	1998–2007
Duration T (years)	7	8	5	8	4	6	10
Number of sinkholes N	1	1	4	15	2	5	1
N/T (year^{-1})	0.143	0.125	0.800	1.875	0.500	0.833	0.100
$\lambda_{min} = N/S_{max}T$ (top number), $\lambda_{max} = N/ST$ (km^{-2} year^{-1})	0.0046 / 0.014	0.0040 / 0.012	0.0258 / 0.08	0.0605 / 0.18	0.0161 / 0.05	0.0269 / 0.08	0.0032 / 0.01
Stability category for values $\lambda_{min}/\lambda_{max}$	V/IV	V/IV	IV/III	III/II	IV/III	IV/III	V/IV
Load cycles	I (1961–1975)		II (1976–1988)		III (1989–2000)		

Stability categories are given in accordance with TSN 22-308-98 NN [29]; $S_{max} = 31$ km^2, $S = 10$ km^2 are the maximal and most likely or effective areas of the zone of influence of the water intake.

cess. This can be readily seen from the obtained data presented as Table 5. Note also that curve *1* in Fig. 10 is based exclusively on observation data; therefore, it takes into account the contribution of the karst process proper (gypsum leaching) to the formation of surface forms.

At the first two stages, the formation frequencies of sinkholes, which are referred to as background natural–technogenic, are $(N/T)_1 = 0.143$ year^{-1} and $(N/T)_2 = 0.125$ year^{-1} (Table 5). At the current stage, we can speak only about background natural or, at least, technogenic–natural development of the process, if we take into account the disturbed properties and the state of soils of the blanket stratum after the three cycles of changes in the hydrodynamic pressure. However, the force technogenic impact has become negligible by 2008. The deterioration of the properties and the state of soils was over and above compensated for by the filling of fracture–pore space of soluble rocks and a decrease in their accumulation capacity, whose value, generally speaking, determines the stability of karst territories [3]. Rock dissolution can increase the accumulation capacity, but it is just the background process mentioned above. Thus, there were no grounds to expect the formation of new collapses in 2008–2010 and the value of $(N/T)_7 = 0.100$ year^{-1} at the seventh stage was interpreted as the maximal possible value of the frequency, which the process would have been characterized, had a new funnel appear in 2008. If this had taken place in 2009 or 2010, the frequency would have been somewhat less, though still close to the maximal value: $(N/T)_7 = 0.091$ year^{-1} and $(N/T)_7 = 0.083$ year^{-1}, respectively.

Overall, data in Table 5 show a close relationship between the three cycles of anthropogenic load and the characteristics that are of importance for the assessment of hazard and risk, such as the frequency N/T and the rate λ of the process. They vividly demonstrate the changes in the category of stability of the territory as a function of λ, maximal (S_{max}), and the most likely or effective (S) area of the water intake influence domain. Note that both the category and the values of λ can be and, seemingly, must be corrected as the result of improvement of the values of S_{max} and S. It is reasonable to carry out a large-scale typological zoning of the territory. It will enable the karst fields and areas to be associated with specific geotechnical conditions and thus, the karst–suffosion hazard and risk to be evaluated with the required degree of detail.

The forecast made in the early 2008 was corroborated during the survey of the area in the spring of 2011: no sinkholes were found to form in 2008–2010. A conical funnel with a depth of $h_c = 1.5$ m was recorded 0.8 km northwest of water intake wells. It formed in late March–early April 2011. Its diameter ($D_c = 3.7$ m) was found to be nearly equal to the forecasted value (Table 4, $(D_c)_{av} = 3.4$ m).

CONCLUSIONS

The geotechnical conditions of the area near Dzerzhinsk City were originally unfavorable for the allocation of industrial and transport facilities because of the hazard of karst formation on land surface. In this area, such hazard manifested itself fully in the second half of the XX century because of the intense withdrawal of groundwater. The accompanying head difference became quite enough to induce the formation of sinkholes, even with no allowance made for the disturbance of hydrochemical regime, which also contribute to the process.

The technogenic impact was especially strong in 1961–1975, when the decolmatation of the fracture–pore space of karst rocks was accompanied by the destruction of low-permeability deposits of urzhumskii stage. These processes created the conditions for the discharge of alluvial sands into fracture–karst collectors and the formation of sinkholes in 1976–1988. In 1989–2000, anthropogenic load onto subsurface hydrosphere decreased significantly, the intermediate

cavities collapsed, open karst cavities were filled, and the rate of the process decreased. Thus, the many-year "experiment" finished favorably: the geological medium persisted, and the frequency and rate of sinkhole formation dropped to their background values. The study and the obtained results suggest the following major conclusions.

1. The geotechnical conditions of the territory are determined by the following features: the carbonate rocks of kazanskii and the gypsums of sakmarskii stages can accumulate crushed connected and loose soils from overlying strata. Collapses and formation of intermediate cavities took place in the overlying low-permeability urzhumskie deposits. The Quaternary sand soils, nearest to land surface, show quicksand properties and suffusion instability.

2. In the last 65 years of the XX century, groundwater regime changed considerably. Intense pumping of subsoil and confined fracture–karst waters caused a drop in their level by 17 m and head by 22 m by the mid-1970s. In 1969 and 1973, the difference between piezometric levels reached 20–25 m and 14–19 m, respectively. Since the second half of the 1990s, the levels have been recovering.

3. Three cycles of changes in the hydrodynamic pressure are identified, lasting for 15, 13, and 12 years and showing gradually decreasing force impact on the rock massif. They are preceded by a stage of 1935–1960, during which the downward hydrodynamic pressure decreased to zero and below it. Two background (natural–technogenic) funnels formed at this stage. Other 27 sinkholes show a distinct relationship between the rate of anthropogenic load and the time distribution of the number, mean size, and the formation frequency of the funnels.

4. During the first cycle, conditions were created for the manifestation of karst–suffosion process on land surface. During the second cycle, the hazard becomes real and reaches its peak, while at the third cycle it decreases and never manifests itself on land surface between 1999 and 2007.

5. In the zone of influence of the water intake, all low permeability rocks of urzhumskii stage were to some extent subject to hydraulic destruction. In the period 1961–2000, through holes in aquiclude could appear not only in water intake area. However, they cannot be expected to form now. Currently, of greatest significance in the stability of the territory are the processes of erosion and redistribution of the filler of fracture–pore space, as well as the discharge of Quaternary sands into karst collectors, i.e., mass suffusion.

6. Under the conditions that have formed by 2008, the diameter of possible sinkholes lies within 2.4–5.0 m with the mean value of 3.4 m. The maximal possible frequency of the process for the most pessimistic scenario of its development is $N/T = 0.1$ year^{-1}, i.e., one sinkhole in 10 years. The forecasted rate of sinkhole formation as a function of the area considered in the water intake influence zone is $\lambda = 0.0032–0.10$ km^{-2} year^{-1}, and the stability category according to [29] is IV–V.

7. The forecast made in the early 2008 was corroborated by the data of field study in the area in the spring of 2011.

REFERENCES

1. Anikeev, A.V., On two forms of destruction of coherent soils over a cavity, *Geoekologiya*, 1993, no. 2, pp. 124–132.
2. Anikeev, A.V., On the causes of collapses and local subsidence of land surface in Moscow, *Geoekologiya*, 2002, no. 4, pp. 363–371.
3. Anikeev, A.V., On the problem of local prediction of stability of karst territories, *Vestn. Mosk. Univ., Ser. 4: Geol.*, 1999, no. 4, pp. 48–56.
4. Anikeev, A.V., Sinkholes in the areas of overlain karst as the result of mass suffusion of sands and destruction of clays, in *Karstovedenie—XXI vek: teoret. i prakt. znachenie: Mater. Mezhdunar. simp. (25–30 maya 2004, Perm', Rossiya)*, (Karst Studies—The XXI Century: Theor. and Pract. Significance: Mater. Intern. Symp. May 25–30, 2004, Perm, Russia), Perm: PGU, 2004, pp. 216–220.
5. Anikeev, A.V., Suffosion: mechanism and kinematics of free suffosion, *Geoekologiya*, 2006, no. 6, pp. 544–553.
6. Baryakh, A.A., Stazhevskii, S.B., Timofeev, E.A., and Khan, G.N., On deformed state of a rock massif over karst cavities, *Fiz.-Tekhn. Probl. Razrab. Polezn. Iskop. (FTPRPI)*, 2008, no. 6, pp. 3–12.
7. *Gruntovedenie* (Soil Science), Trofimov, V.T., Ed., Moscow: MGU, 2005.
8. Zverev, V.P., *Gidrogeokhimicheskie issledovaniya sistemy gipsy–podzemnye vody* (Hydrogeochemical Studies of Gypsum–Groundwater System), Moscow: Nauka, 1967.
9. Zverev, V.P., Hydrogeochemical methods of gypsum karst studies, in *Proektirovanie, stroitel'stvo i ekspluatatsiya zemlyanogo polotna*, no. 8 (*Tr. soveshchaniya v g. Gor'kom v oktyabre 1965 g.*) (Designing, Construction, and Operation of Roadbeds, no. 8 (Proc. Meeting in Gorky C. in October 1965)), Moscow: Transport, 1968, pp. 44–50.
10. Il'in, A.N., Kapustin, A.P., Kogan, I.A., et al., *Karstovye yavleniya v raione g. Dzerzhinska Gor'kovskoi oblasti* (Karst Phenomena near Dzerzhinsk C., Gorky oblast), Moscow: AN SSSR, 1960.
11. *Istoriya predpriyatiya "Protivokarstovaya i beregovaya zashchita." 55-letie deyatel'nosti, 1952–2007* (History of the Institution OAO Antikarst and Shore Protection, 55-year Activity, 1952–2007), Ikonnikov, L.B. and Tolmachev, V.V., Eds., Dzerzhinsk: OAO Dzerzhinskaya tipografiya, 2007.
12. Kazikaev, D.M., *Geomekhanicheskie protsessy pri sovmestnoi i povtornoi razrabotke rud* (Geomechanical Processes in Combined and Repeated Development of Ores), Moscow: Nedra, 1981.
13. Keneman, F.E., On free outflow of granular solids, *Izv. AN SSSR. OTN. Mekh. Mashinostr.*, 1960, no. 2, pp. 70–77.

14. Klein, R.G., *Stroitel'naya mekhanika sypuchikh tel* (Construction Mechanics of Granular Solids), Moscow: Stroiizdat, 1977.

15. Kramadzhyan, A.A., Lindkvist, P.-A, Manson, A., et al., On the forms of flow domains in granular materials at their release, *Fiz.-Tekhn. Probl. Razrab. Polezn. Iskop. (FTPRPI)*, 1994, no. 2, pp. 34–46.

16. Kulikov, V.V., *Sovmestnaya i povtornaya razrabotka rudnykh mestorozhdenii* (Joint and Repeated Development of Ore Deposits), Moscow: Nedra, 1972.

17. Kul'chitskii, L.I. and Gabibov, F.G., *Issledovanie zakonomernostei izmeneniya svoistv lessovykh suglinkov pri izmenyayushchemsya vlazhnostnom rezhime (mikroreologicheskii podkhod)* (Studying Regularities of Changes in the Properties of Loess Loams under Changing Moisture Regime: Microrheological Approach), Baku: Adil'ogly, 2004.

18. Lin'kov, A.M., Numerical modeling of fluid flow and hydrofracture propagation, *Fiz.-Tekhn. Probl. Razrab. Polezn. Iskop. (FTPRPI),* 2008, no. 1, pp. 26–46.

19. Lin'kov, A.M. and Petukhov, I.M., On the theory of coal bed destruction by layer-by-layer tearing-off, *Gornoe davlenie i gornye udary. Tr. VNIMI* (Ground Pressure and Rock Bumps, Trans. VNIMI), 1973, Coll. 88, pp. 205–221.

20. Makarova, V.N., Balashova, T.A., and Sukhanova, T.V., On the role of suffusion in the formation of subsidence forms in Nizhneokskii district, *Vestn. Mosk. Univ., Ser. 4: Geol.*, 1998, no. 2, pp. 60–65.

21. Nikol'skii, A.A., On waves of sudden outburst of gas-containing rocks, *Dokl. Akad. Nauk SSSR,* 1953, vol. 88, no. 4, pp. 572–582.

22. Petukhov, I.M. and Lin'kov, A.M., *Mekhanika gornykh udarov i vybrosov* (Mechanics of Rock Bumps and Outbursts), Moscow: Nedra, 1983.

23. Pokrovskii, G.I. and Aref'ev, A.I., On the discharge of granular solids, *Zh. Tekh. Fiz.*, 1937, vol. 7, no. 4, pp. 424–427.

24. Rusin, E.P., Stazhevskii, S.B., and Khan, G.N., Geometric aspects of the genesis of exo- and endokarst, *Fiz.-Tekhn. Probl. Razrab. Polezn. Iskop. (FTPRPI),* 2007, no. 2, pp. 10–20.

25. Savarenskii, I.A., Geotechnical assessment of karst phenomena near Dzerzhinsk C., in *Voprosy izucheniya karstovykh yavlenii v raione g. Dzerzhinska: Tr. LGGP* (Issues of Studying Karst Phenomena near Dzerzhinsk C.), Moscow: AN SSSR, 1962, vol. 47, pp. 12–26.

26. Stazhevskii, S.B., On the first form of granular material flow in bins, *Fiz.-Tekhn. Probl. Razrab. Polezn. Iskop. (FTPRPI)*, 1983, no. 3, pp. 14–21.

27. Stazhevskii, S.B., On the form of granular material flow in bins, *Fiz.-Tekhn. Probl. Razrab. Polezn. Iskop. (FTPRPI)*, 1985, no. 5, pp. 3–16.

28. Tolmachev, V.V. and Roiter, F., *Inzhenernoe karstovedenie* (Engineering Studies of Karst), Moscow: Nedra, 1990.

29. *TSN 22-308-98 NN. Inzhenernye izyskaniya, proektirovanie, stroitel'stvo i ekspluatatsiya zdanii i sooruzhenii na zakarstovannykh territoriyakh Nizhegorodskoi oblasti* (Engineering Surveys, Design, Construction, and Operation of Buildings and Structures in Karst Areas in Nizhegorodskaya Oblast), Administratsiya Nizhegorodskoi obl., Komitet arkhitektury i gradostroitel'stva, Nizhni Novgorod, 1999.

30. Khomenko, V.P., *Karstovo-suffozionnye protsessy i ikh prognoz* (Karst–Suffosion Processes and Their Forecasting), Moscow: Nauka, 1986.

31. Khomenko, V.P., *Zakonomernosti i prognoz suffozionnykh protsessov* (Regularities and Forecasts of Suffosion Processes), Moscow: GEOS, 2003.

32. Khristianovich, S.A., On outburst wave, *Izv. AN SSSR. OTN. Mekh. Mashinostr.*, 1953, no. 12, pp. 1679–1688.

33. Khristianovich, S.A., On disintegration wave, *Izv. AN SSSR. OTN. Mekh. Mashinostr.*, 1953, no. 12, pp. 1689–1699.

34. Khristianovich, S.A., Gas pressure distribution near a moving free coal surface, *Izv. AN SSSR. Mekh. Mashinostr.*, 1953, no. 12, pp. 1673–1678.

35. Khristianovich, S.A., Transient fluid flow in a porous medium at abrupt changes over time or large porosity gradients, *Fiz.-Tekhn. Probl. Razrab. Polezn. Iskop. (FTPRPI),* 1985, no. 1, pp. 3–18.

36. Chernykh, V.A., *Gidrogeomekhanika neftegazodobychi* (Hydrogeomechanics of Oil and Gas Production), Moscow: VNIIGAZ, 2001.

37. Shlykov, V.G., *Rentgenovskii analiz mineral'nogo sostava dispersnykh gruntov* (X-Ray Analysis of the Mineral Composition of Disperse Soils), Sokolov, V.N., Ed., Moscow: GEOS, 2006.

38. Brown, R.L., Minimum energy theorem for flow of dry granules through apertures, *Nature*, 1961, vol. 191, no. 4787, pp. 458–461.

39. Firewicz, H., Kinematics of the gravity flow of granules from a bin—part 5, *Aufbereitungs-Technik*, 1990, vol. 31, no. 2, pp. 79–88.

40. Michalowski, R.L., Strain localization and periodic fluctuations in granular flow processes from hoppers, *Géotechnique*, 1990, vol. 40, no. 3, pp. 389–403.

41. Tharp, T.M., Poroelastic analysis of cover-collapse sinkhole formation by piezometric surface drawdown, *Environ. Geol.*, 2002, no. 42, pp. 447–456.

42. Tuzun, U. and Nedderman, R.M., Experimental evidence supporting kinematic modelling of the flow of granular media in the absence of air drag, *Powder Technol.*, 1979, vol. 24, no. 2, pp. 257–266.

Translated by G. Krichevets